

# AIP | Conference Proceedings

## A hierarchical model for cross-scale simulation of granular media

Ning Guo and Jidong Zhao

Citation: *AIP Conf. Proc.* **1542**, 1222 (2013); doi: 10.1063/1.4812158

View online: <http://dx.doi.org/10.1063/1.4812158>

View Table of Contents: <http://proceedings.aip.org/dbt/dbt.jsp?KEY=APCPCS&Volume=1542&Issue=1>

Published by the [AIP Publishing LLC](#).

---

### Additional information on AIP Conf. Proc.

Journal Homepage: <http://proceedings.aip.org/>

Journal Information: [http://proceedings.aip.org/about/about\\_the\\_proceedings](http://proceedings.aip.org/about/about_the_proceedings)

Top downloads: [http://proceedings.aip.org/dbt/most\\_downloaded.jsp?KEY=APCPCS](http://proceedings.aip.org/dbt/most_downloaded.jsp?KEY=APCPCS)

Information for Authors: [http://proceedings.aip.org/authors/information\\_for\\_authors](http://proceedings.aip.org/authors/information_for_authors)

### ADVERTISEMENT



AIP Advances

*Submit Now*

Explore AIP's new  
open-access journal

- Article-level metrics now available
- Join the conversation! Rate & comment on articles

# A Hierarchical Model for Cross-scale Simulation of Granular Media

Ning Guo and Jidong Zhao

*Hong Kong University of Science and Technology, Clearwater Bay, Kowloon, Hong Kong*

**Abstract.** This paper presents a multiscale modeling framework for granular media based on a hierarchical cross-scale approach. The overall material is treated as a continuum on the macroscale and the corresponding boundary value problem is solved by finite element method (FEM). At each Gauss point of the FEM mesh, a discrete element assembly is embedded from which the material behavior is obtained for the global FEM computation. It is demonstrated that this technique may capture the salient macroscopic behavior of granular media in a natural manner, and meanwhile helps to bypass the conventional phenomenological nature of continuum modeling approaches. Moreover, the framework provides us with rich information on the particle level which can be closely correlated to the macroscopic material response and hence helps to shed lights on the cross-scaling understanding of granular media. Specific linkages between the microscopic origins and mechanisms and the macroscopic responses can be conveniently developed. As a demonstrative example, the strain localization of granular sand in biaxial compression test is investigated by the multiscale approach to showcase the above features.

**Keywords:** hierarchical multiscale modeling; finite/discrete element methods; granular media; strain localization

**PACS:** 61.43.-j; 83.80.Fg; 83.50.Ax; 45.70.Vn

## INTRODUCTION

Granular matter transmits forces through interparticle contacts and forms highly inhomogeneous contact force network inside the system to balance the external force [1, 2]. Seemingly simple on each individual particle, the inherent and induced inhomogeneity and the microscopic self-reorganization of the entire system lead to a complex collective behavior at the macroscopic level, including state-dependent dilatancy, non-coaxiality, and strain localization [3, 4, 5]. The development of a robust constitutive model to capture all or even some of these aspects of granular media proves to be challenging. Recently, the discrete element method (DEM) has become a popular tool in many areas to investigate the behavior of granular media. DEM respects the discrete nature of granular media and models the material system as an assembly of interacted individual particles. Based often on rather simple contact law at microscopic level, DEM has been demonstrated to be capable of capturing many salient macroscopic features of granular media and meanwhile providing interesting insights into the evolution of the associated internal micro-structures [6, 7, 8, 9].

One of the biggest constraints of DEM simulation of granular media lies in its limitation in modeling very large scale systems with realistic particle size, e.g., practical engineering level problems. To address this issue, considerable efforts have been paid by researchers in the community of granular mechanics and computational mechanics to develop coupled approach to combine the continuum level simulations and the discrete-based methods. Special focus has been placed on de-

veloping effective ways to link the microscopic origins and mechanisms of granular media with their overall mechanical behavior, or so-called micro-macro bridging through homogenization techniques [10, 11]. The concept and the methodology are further extended to a hierarchical cross-scale framework [12, 13, 14] to solve true boundary value problems (BVPs) where the macroscopic responses are homogenized from microscopic discrete data, thus the constitutive law is no longer required. In line with this, the study is devoted to develop a cross-scale modeling framework for granular material modeling. In this approach, the finite element method (FEM) is used to tackle the large scale BVPs by virtue of its computational efficiency. At each Gauss point of the FEM domain, a discrete element assembly is embedded to serve as a representative volume element (RVE) which is the smallest unit that efficiently captures the material constitutive behavior with sufficient accuracy. To elaborate, the material point response is computed by receiving boundary conditions from the FEM domain and then passed on to the Gauss point for the FEM calculations. In so doing, no constitutive assumptions, which are frequently criticized to be phenomenological in nature, are needed *a priori* for the continuum modeling. In what follows, the solution procedure and formulations of the hierarchical multi-scale modeling framework are first introduced. The predictive capability of this framework is then demonstrated by the examination of a biaxial compression test on granular sand wherein strain localization is observed. Throughout the paper, if not otherwise stated, indicial tensor notation and Einstein summation convention are used.

## SOLUTION PROCEDURE

In a typical displacement-driven FEM, the global governing equation is solved by first discretizing the considered domain into finite mesh in which the local displacement and strain increments are interpolated from boundary conditions. At each Gauss point, an incremental constitutive relation is then required to link the strain increment with the stress increment:

$$\dot{\sigma}_{ij} = D_{ijkl} \dot{\epsilon}_{kl} \quad (1)$$

where  $\mathbb{D}$  denotes the tangent operator. The infinitesimal strain is calculated by:

$$\epsilon_{ij} = \frac{1}{2}(u_{i,j} + u_{j,i}) \quad (2)$$

where  $\vec{u}$  is the unknown displacement vector. A linear elastic problem can be solved directly since  $\mathbb{D}$  is indeed the elastic modulus. For a general nonlinear case, Newton-Raphson method is usually used to solve the problem iteratively.

Instead of assuming a phenomenological constitutive model *a priori*, we perform DEM simulations to obtain the material behavior at each Gauss point. The boundary condition for a particular DEM RVE is extracted from the deformation field of the FEM domain at the specific Gauss point. The homogenized stress and tangent operator are then returned to the global FEM equation. Iterative schemes are employed to find a converged solution. The procedure is summarized below:

1. Find a trial solution using the current stress and tangent operator.
2. Use the solution as boundary condition for each RVE and update stress and tangent operator.
3. Repeat the above steps until convergence is reached.

## DEM and Homogenization

An popular open-source code YADE [15] has been used for the DEM part of the multiscale computation. A linear force-displacement contact law is chosen in conjunction with the Coulomb's friction criterion in the DEM to describe the interparticle contacts. The normal stiffness  $k_n$  and the tangential stiffness  $k_t$  are determined from two input parameters  $E_c$  and  $\nu_c$ :

$$k_n = E_c r, \quad k_t = \nu_c k_n \quad (3)$$

where  $r = 2r_1 r_2 / (r_1 + r_2)$  is the common radius of the two particles in contact. A threshold for the tangential (frictional) force  $f_t^c$  is imposed:

$$|f_t^c| \leq f_n^c \tan \varphi \quad (4)$$

where  $f_n^c$  is the normal contact force,  $\varphi$  is the interparticle friction angle. A simple local non-viscous damping force [16] is also added to ensure quasi-static condition:

$$f_i^{\text{damp}} = -\alpha \text{sign}(v_i) |f_i^{\text{resid}}| \quad (5)$$

where  $\alpha$  is the damping ratio,  $\vec{v}$  is the velocity of the particle, and  $\vec{f}^{\text{resid}}$  is the residual force summed over all contacts on the particle.

The homogenized Cauchy stress tensor for a DEM packing follows the Love formula [17, 18]:

$$\sigma_{ij} = \frac{1}{V} \sum_{N_c} f_i^c d_j^c \quad (6)$$

where  $V$  is the total volume (or area in two-dimension) of the packing,  $N_c$  is summed contact number within the packing,  $\vec{f}^c$  is the contact force, and  $\vec{d}^c$  is the branch vector connecting centers of the two contact particles. Two commonly referred quantities in soil mechanics – the mean effective stress  $p$  and the deviatoric stress  $q$  in 2D case are then calculated:

$$p = \frac{1}{2} \sigma_{ii}, \quad q = \sqrt{\frac{1}{2} s_{ij} s_{ij}} \quad (7)$$

where  $\mathbf{s}$  is the deviatoric stress tensor  $s_{ij} = \sigma_{ij} - p \delta_{ij}$  with  $\delta$  being the Kronecker delta. The involved strain quantities are deviatoric strain  $\epsilon_q$  and volumetric strain  $\epsilon_v$ , calculated from the strain tensor  $\boldsymbol{\epsilon}$ :

$$\epsilon_q = \sqrt{2 e_{ij} e_{ij}}, \quad \epsilon_v = \epsilon_{ii} \quad (8)$$

where  $e_{ij} = \epsilon_{ij} - 1/2 \epsilon_{kk} \delta_{ij}$ .

We use the homogenized bulk elastic modulus of the packing as a first trial approximation of the tangent operator. The analytical form is derived based on the assumption of uniform strain field [19, 20, 12]:

$$D_{ijkl} = \frac{1}{V} \sum_{N_c} (k_n n_i^c d_j^c n_k^c d_l^c + k_t t_i^c d_j^c t_k^c d_l^c) \quad (9)$$

where  $\vec{n}^c$  and  $\vec{t}^c$  are the unit vectors in the normal and tangential directions at a contact.

## Representative Volume Element

It remains debatable how large a proper RVE should be chosen. Generally the size of the RVE should be large enough to be statistically representative and meanwhile adequately compact to render it computationally effective. In the current study, the parameters and the RVE size are calibrated such that the behavior of the RVE is in qualitatively consistent with the laboratory data on sand.

**TABLE 1.** Parameters for the DEM model

| Radii (mm) | Density (kg/m <sup>3</sup> ) | $E_c$ (MPa) | $\nu_c$ | $\phi$ (rad) | $\alpha$ |
|------------|------------------------------|-------------|---------|--------------|----------|
| 1-3        | 2650                         | 100         | 0.7     | 0.5          | 0.2      |

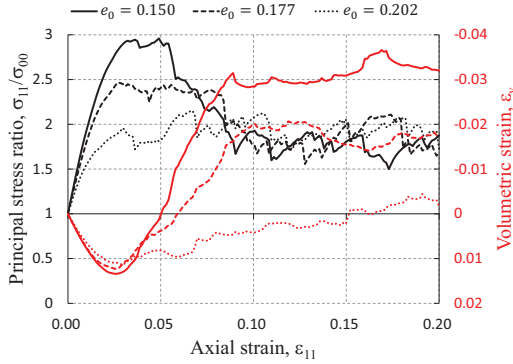


**FIGURE 1.** Behaviour of the calibrated RVE

The RVE finally calibrated contains 2000 polydisperse circular particles (cylindrical rods) with a mean radius  $r_{\text{mean}} = 2$  mm. Selected parameters for the DEM model are presented in Table 1. Periodic boundary applies in both directions of the DEM assembly with zero gravity (i.e., no body force). We first examine the behavior of the RVE in drained biaxial compression with an initial isotropic pressure ( $p_0 = 300$  kPa) but different void ratios  $e_0$ . From Fig. 1, it is found that dense packing has larger peak strength and is more dilatative than the loose packing. The three cases shown are consistent with typical behavior of dense, medium dense and loose samples of sand. The same RVE is used in the following multi-scale modeling of the biaxial compression problem.

## BIAXIAL COMPRESSION TEST

A sample of  $100\text{ mm} \times 200\text{ mm}$  under biaxial compression is considered. The domain is discretized into  $6 \times 10$  first-order quadrilateral (Q1) elements. The mesh and the boundary condition are illustrated in Fig. 2. An identical dense packing of RVE is attached to each Gauss point. The specimen is loaded in the vertical direction with a constant confining pressure  $\sigma_{00} = 300$  kPa applied to the horizontal.

Fig. 3(a) shows the deviatoric strain contour at a global axial strain about 0.5% when a localized deformation is initiated. Since all boundary conditions and the applied loads are symmetric, and the material properties and initial state are homogeneous in the sample as well. Conventional FEM simulation would other predict no occurrence of localization at all. However, the current multi-

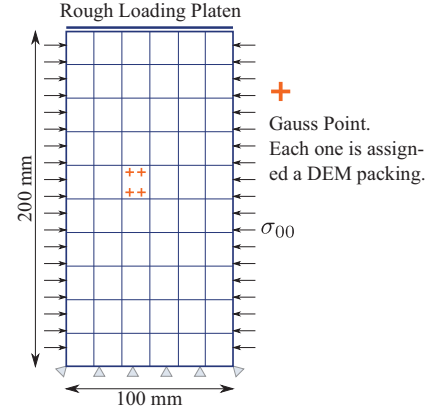


**FIGURE 2.** Discretization and boundary condition of the specimen

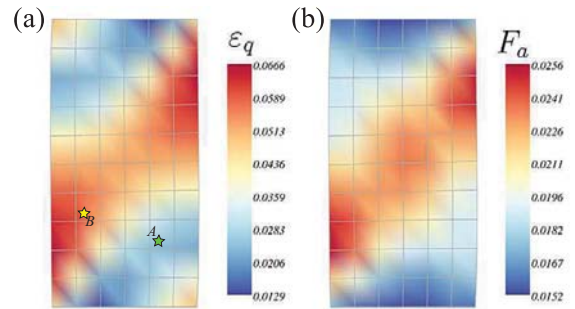


**FIGURE 3.** Contour of (a) deviatoric strain; (b) fabric anisotropy

scale simulation shows that the initially identical RVEs at different Gauss points evolve along different loading paths, which results in different fabric. The asymmetric physical fabric breaks the symmetry of the sample and causes asymmetric localization. Our modeling thus shows that the occurrence of localization is a result of material behavior rather than arbitrary perturbations reported in many other studies.

Indeed, by virtue of the multi-scale modeling approach, the overall material response can be directly linked to the underlying microstructure and the microscopic mechanism. One quantity reflecting the microstructure is the so-called fabric tensor. The contact-normal based fabric tensor proposed by [21] is employed here:

$$\phi_{ij} = \frac{1}{N_c} \sum_{N_c} n_i^c n_j^c \quad (10)$$

The trace of  $\phi$  is  $\phi_{ii} = 1$ . A deviatoric tensor can be calculated which quantifies the fabric anisotropy:

$$F_{ij} = 4(\phi_{ij} - \frac{1}{2}\delta_{ij}) \quad (11)$$

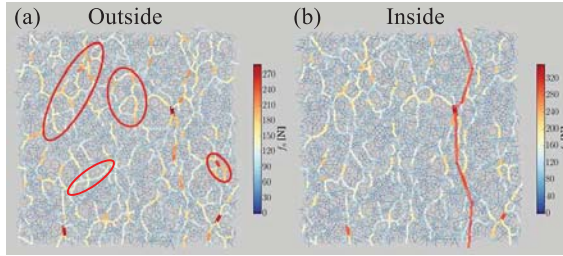


**FIGURE 4.** Contact force network for RVEs (a) outside and (b) inside the localized region

The second invariant of  $F_{ij}$  is used to measure the anisotropic intensity  $F_a = \sqrt{1/2 F_{ij} F_{ij}}$ . Fig. 3(b) shows the contour of  $F_a$  over the problem domain. Notably, the localized region is more anisotropic than the surrounding region due to concentrated shearing.

The local structure characteristics are further examined from the contact force network of the RVEs. Fig. 4 shows a comparison between two RVEs, one located outside and the other inside of the strain localized region, corresponding to Point A and B in Fig. 3(a) respectively. As can be seen, the contact forces are larger and more concentrated within the localized region with the anisotropic orientation mainly aligned in the compression direction (indicated by a thick line), while the surrounding force chains are weakened (indicated by ellipses) which makes the penetrating strong force chains fragile to buckling [see also 22, 23].

## CONCLUSIONS

We developed a hierarchical cross-scale framework and extended it to solve a boundary value problem for granular media. The method may help to bypass the phenomenological way in conventional constitutive modeling, and meanwhile offers rich information linked to the microscopic level of the material. An example of strain localization in biaxial compression test was used to demonstrate this feature. We note that, however, the proposed method is computationally expensive. Coarse mesh has been used in the demonstrated example, and the computation has been terminated by rather small strain level, e.g., the initiation of localization. Due to fluctuations in simulated responses by DEM, the numerical scheme may not converge in some cases. As an ongoing work, we are still working on such aspects as parallelization of the RVE computations and design of robust iterative schemes to improve the method.

## ACKNOWLEDGMENTS

This study was supported by RGC/GRF 623609.

## REFERENCES

1. F. Radjai, D. E. Wolf, M. Jean, and J. J. Moreau, *Physical Review Letters* **80**, 61–64 (1998).
2. H. Ouadfel, and L. Rothenburg, *Mechanics of Materials* **33**, 201–221 (2001).
3. X. S. Li, *Géotechnique* **52**, 173–186 (2002).
4. M. Gutierrez, and K. Ishihara, *Soils and Foundations* **40**, 49–59 (2000).
5. H. Muhlhaus, and I. Vardoulakis, *Géotechnique* **37**, 271–283 (1987).
6. C. Thornton, *Géotechnique* **50**, 43–53 (2000).
7. L. Rothenburg, and N. Kruyt, *International Journal of Solids and Structures* **41**, 5763–5774 (2004).
8. C. O’Sullivan, *Particulate Discrete Element Modelling: A Geomechanics Perspective*, Taylor & Francis, 2011.
9. N. Guo, and J. Zhao, *Computers and Geotechnics* **47**, 1–15 (2013).
10. V. Kouznetsova, M. G. D. Geers, and W. A. M. Brekelmans, *International Journal for Numerical Methods in Engineering* **54**, 1235–1260 (2002).
11. C. Miehe, J. Dettmar, and D. Zäh, *International Journal for Numerical Methods in Engineering* **83**, 1206–1236 (2010).
12. H. Meier, P. Steinmann, and E. Kuhl, “On the Multiscale Computation of Confined Granular Media,” in *ECCOMAS Multidisciplinary Jubilee Symposium*, edited by J. Eberhardsteiner, C. Hellmich, H. Mang, and J. Périaux, Springer Netherlands, 2009, vol. 14 of *Computational Methods in Applied Sciences*, pp. 121–133.
13. J. Andrade, C. Avila, S. Hall, N. Lenoir, and G. Viggiani, *Journal of the Mechanics and Physics of Solids* **59**, 237–250 (2010).
14. M. Nitka, G. Combe, C. Dascalu, and J. Desrues, *Granular Matter* **13**, 277–281 (2011).
15. V. Šmilauer, A. Gladky, J. Kozicki, C. Modenese, and J. Stránský, “Yade Using and Programming,” in *Yade Documentation*, edited by V. Šmilauer, The Yade Project, 2010, 1st edn.
16. P. A. Cundall, and R. Hart, *Engineering Computations* **9**, 101–113 (1992).
17. A. E. H. Love, *A Treatise on the Mathematical Theory of Elasticity*, Cambridge University Press, Cambridge, 1927.
18. J. Christoffersen, M. M. Mehrabadi, and S. Nemat-Nasser, *Journal of Applied Mechanics* **48**, 339–344 (1981).
19. N. Kruyt, and L. Rothenburg, *International Journal of Engineering Science* **36**, 1127–1142 (1998).
20. S. Luding, *International Journal of Solids and Structures* **41**, 5821–5836 (2004).
21. M. Satake, “Fabric tensor in granular materials,” in *IUTAM symposium on Deformation and Failure of Granular Materials*, A.A. Balkema, Delft, 1982, pp. 63–68.
22. M. Oda, and K. Iwashita, *International Journal of Engineering Science* **38**, 1713–1740 (2000).
23. A. Tordesillas, *Philosophical Magazine* **87**, 4987–5016 (2007).